ELSEVIER

Earth and Planetary Science Letters 171 (1999) 277–287

EPSL

www.elsevier.com/locate/epsl

Comparison of flat-topped stellate seamounts on Earth's seafloor with stellate domes on Venus using side-scan sonar and Magellan synthetic aperture radar

M.H. Bulmer [a,*], J.B. Wilson [b]

[a] *Center for Earth and Planetary Studies, National Air and Space Museum, Smithsonian Institution, Washington, DC 20560, USA*
[b] *Department of Geology, Royal Holloway, University of London, Egham, Surrey, TW20 OEX, UK*

Received 14 September 1998; revised version received 30 April 1999; accepted 21 June 1999

Abstract

The diameters of many domes on Venus imaged by the Magellan synthetic aperture radar (SAR) are an order of magnitude larger than terrestrial subaerial domes; however, surveys of the seafloor using sonar imaging systems such as GLORIA (Geological Long Range Inclined Asdic) and SeaBEAM have revealed flat-topped volcanic features with similar diameters, volumes and slope angles. Suggested analogies between domes on Venus and seamounts on the northern East Pacific Rise and off Hawaii have been tested by D.K. Smith [J. Volcanol. Geotherm. Res. 73 (1996) 47–64] using comparisons of size and shape and significant differences identified. GLORIA images of flat-topped seamounts near Hawaii show them to have stellate planforms. Over half of the total population of 375 domes on Venus have been modified and many have stellate planforms. We have focused on the similarities in stellate planforms between flat-topped seamounts and modified domes on Venus. We have used GLORIA sonar and Magellan radar data to constrain the formation and evolution of both flat-topped seamounts on the ocean floor and volcanic domes on Venus to see if the processes that formed them are similar. We propose that flat-topped seamounts on the Hawaiian Ridge are built on sediments overlying the oceanic crust and that available evidence supports three processes that can form stellate margins: (1) radial dike intrusions related to flank rift zones; (2) dike intrusions which cause slope failures; and (3) gravitational slope failures unrelated to intrusions. For Venus, where low erosion rates and the absence of a sediment layer results in lavas being emplaced directly onto the crust, the available evidence supports stellate margins originating by gravitational slope failures unrelated to diking, though intrusions cannot be ruled out with existing data.

Keywords: seamounts; Earth; domes; Venus; side-scanning methods

1. Introduction

During the GLORIA side-scan survey around the Hawaiian Islands (U.S. Exclusive Economic Zone mapping project) conducted jointly by the United States Geological Survey and the Institute of Oceanographic Sciences (UK) in the 1980s, images were obtained of seamounts with stellate planforms and flat tops [1]. Images acquired during the Magellan Mapping Mission to Venus showed volcanic features that also possess stellate planforms and near-horizontal upper surfaces. Analogies made between domes on Venus and seamounts on the northern East Pacific

* Corresponding author. Tel.: +1-202-633-9896; Fax: +1-202-786-2566; E-mail: mbulmer@ceps.nasm.edu

0012-821X/99/$ – see front matter
PII: S0012-821X(99)00154-5

Rise [2] and off Hawaii [3] have been tested using comparisons of size and shape [4]. The results of this comparison showed that seamounts were more analogous to Venusian shields and cones [5,6] than to domes. The comparison of size and shape of Venus domes was made with the total spectrum of seamount morphologies. We have focused on the similarities in stellate planforms between flat-topped seamounts on the Hawaiian Ridge from 18°N to 31°N [1,7] and modified domes on Venus [8], to examine whether the processes that formed them on the seafloor and on Venus are similar. Seamount data are compared with results from a global examination of both modified and unmodified volcanic domes on Venus [5].

As detailed by Smith [4], high surface pressures and rapid initial cooling rates of lavas are the principal similarities between eruptive conditions on the seafloor and on Venus. Surface pressure is important in edifice morphology because high pressures inhibit the exsolution of volatiles and fragmentation, which in turn effects lava bulk density. At typical water depths around the Hawaiian Ridge of 2000–3000 m, the pressure is 20–30 MPa. On Venus, the pressure in the lowest part of the plains is 9.5 MPa and at the highest elevations that domes are found is 9 MPa. The temperature differential between fresh lavas and seawater causes rapid quenching. A similar effect occurs on Venus because of the rapid convective cooling into the dense CO_2-rich atmosphere [9]. The majority of seamounts are predominantly composed of tholeiitic basalts [10]. On Venus, a range of magma compositions has been proposed for domes, which includes rhyolites and dacites [11–15]. However, domes on Venus lack the progression in surface morphologies, and the topographic variability of terrestrial rhyolitic and dacitic domes on Earth [16]. Aside from evolved lavas, highly viscous magma rheologies may also rise from a high volume percent of crystals [11] or a high volatile content [17]. Using controlled laboratory simulations, Gregg and Fink [18] showed that the formation of domes requires an effusion rate of $<10^{-6}$ m^3/s if a basaltic composition ($\eta = 10^2$ Pa s) is assumed, or a maximum of 10 m^3/s if an andesitic composition ($\eta = 10^6$ Pa s) is used.

2. Sonar and radar instruments

GLORIA is a low-frequency (~6.5 kHz FM) side-scan sonar (Table 1) operating at a 22 cm wavelength [19]. The strength of the acoustic backscatter is primarily a function of: (1) the slope orientation relative to the incident sonar signal; (2) the surface roughness factor [20]; (3) the variation in physical properties of the upper few meters of the seafloor; and (4) the characteristics of the water column which attenuates the strength of the sonar signal as well as produces background noise. Additional seafloor data collected simultaneously with the GLORIA side-scan sonar around Hawaii included bathymetry, acoustic-reflection profiles, echo soundings, magnetics and gravity signatures [21].

Magellan's radar system operated at a 12.6 cm wavelength and collected synthetic aperture radar SAR images, radar altimetry and radiometry data [22]. The spatial resolution of the SAR is comparable to GLORIA sonar resolution (Table 1). Similar to GLORIA, brightness variations in Magellan images result from large-scale surface topography, wavelength-scale roughness and the electrical prop-

Table 1
Characteristics of GLORIA sonar and Magellan SAR instruments

	GLORIA sonar	Magellan radar
Frequency band	–	S
Wavelength	22 cm	12.6 cm
Operating frequency	Port 6.8 kHz and starboard array 6.2 kHz	2.38 GHz
Polarization	–	HH
Incidence angle	10–90°	15–45°
Antenna	5.3 m long by 40 cm high	3.7 m (dish)
Effective slant-range resolution	50 m	88 m
Along-track resolution	120 m	125 m
Swath width	20–25 km	45 km

erties of the upper layers of the surface. The relative effects of changes in these parameters are a function of incidence angle, direction of illumination and imaging wavelength. Empirical links have been made between the Magellan SAR backscatter and surface roughness [23] but this is not the case for the GLORIA sonar [24], prohibiting any quantitative comparisons between the two data sets. For both GLORIA and Magellan data sets presented here, high backscatter is represented by bright tones and low backscatter by dark tones. Terrain that slopes toward the imaging system has a bright tone and is compressed relative to terrain that slopes away, which has a dark tone and is spatially expanded. In the absence of topographic effects, surface roughness at the scale of the sensor wavelength may dominate the backscatter.

3. Observations of flat-topped seamounts

The systematic GLORIA side-scan survey around the Hawaiian Islands revealed numerous seamount morphologies [1,7,21]. We focused our attention on flat-topped seamounts, particularly those with stellate planforms rather than cones, small shields, or larger volcanic constructs. Measurements of seamounts were made using the full resolution GLORIA image data (50 m/pixel). Flat-topped seamounts range in diameter between 10 and 60 km, have steep, rough (at the sonar wavelength) flanks, stellate planforms and sonar-dark (low backscatter) flat summit areas with occasional central craters (Fig. 1). As well as these flat-topped seamounts there are two other categories of seamounts which are both <10 km in diameter. The first are circular and typically 400–500 m high, with steep flanks that rise to flat upper surfaces often with a summit crater (Fig. 1), and the second category are non-circular and have rough surface textures at the scale of the sonar wavelength. To understand the different seamounts morphologies around the Hawaiian Ridge it is important to examine the magmatic and tectonic environment. Seamounts adjacent to the Hawaiian Ridge will have been exposed to stresses which include earthquake loading, crustal subsidence and arching parallel to the main axis of the ridge, and partial volcanic overprinting by the propagating Hawaiian hotspot [1]. Flat-topped seamounts probably Cretaceous in age

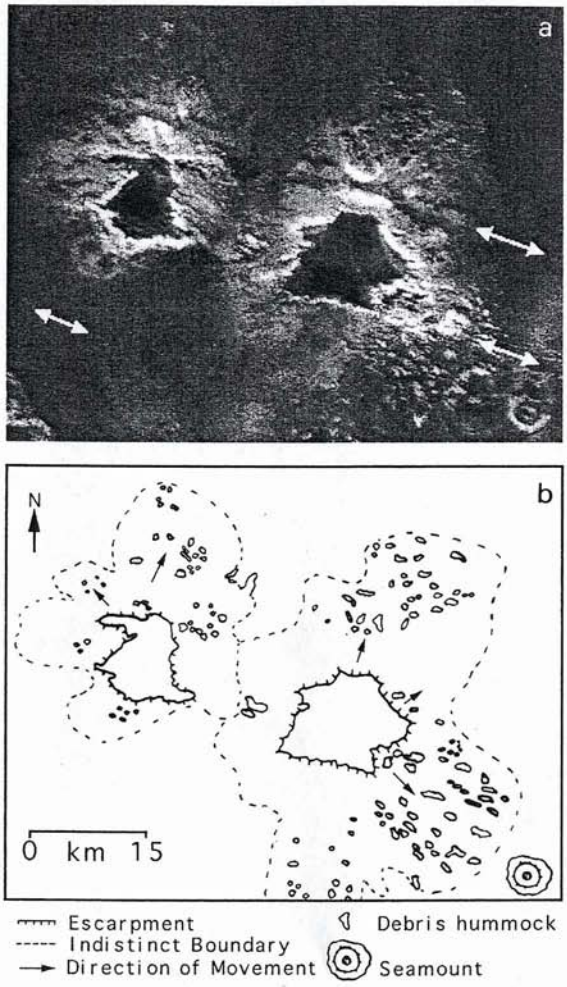

Fig. 1. Two flat-topped seamounts with stellate planforms and diameters between 15 and 10 km located on the central Hawaiian Ridge (27°N, 168°W). GLORIA image and sketch map show the aprons of high backscatter material surrounding the seamounts. The lobate apron off the southeast flank of the eastern seamount traveled 15 km and has hummocky terrain in the toe. The apparent elongation of hummocks parallel to ship tracks (shown by white arrows) is an artifact. A smaller circular seamount is situated to the southeast of the larger flat-topped seamount. The sonograph images represent orthorectified and true plan views (assuming a flat seafloor) of acoustic backscatter patterns on the seafloor either side of the ship tracks. USGS/IOS EEZ GLORIA image H2q39 and H2q40.

(73–106 Ma) occur in isolation on seafloor formed between 95 and 128 Ma [21], and also in clusters such as those located south of the main axis of the Hawaiian chain between 173°W, 24°N and 174°W,

25°N. Some clusters of seamounts imaged by GLORIA form chains such as those at 168°W, 27°N to the northwest of the Gardner Pinnacles, suggesting that they formed along fractures which are not visible in the sonar data, possibly due to sediment thickness or overprinting by the edifices themselves.

4. Observations of domes on Venus

Venusian volcanic domes are distinct from other volcanic constructs on the surface of the planet such as shields, cones and large volcanic centers [6,25]. Domes are characterized by short, steep radar-bright convex slopes that often rise to a near-horizontal upper surface. We have identified 375 domes on Venus, 225 more than the 154 found in a previous study [17]. The reason for the difference in number is based on recognition that domes undergo modification from their original circular planform [8]. Of the total of 375 domes on Venus, 316 are irregular often with arcuate or stellate margins (Fig. 2), herein after referred to as modified domes. The remaining 59 domes are circular which are considered to have been unaltered since emplacement [5]. The sizes of domes were measured from the full resolution radar images (75 m/pixel) which have variable incidence angles and look-directions. There are five different morphological categories of modified domes distinguishable by size, planform, and morphology. Those in the first category range in diameter from 15 to 30 km, often have arcuate scarps and have steep flanks that rise to large central craters on the order of 5 km in diameter. Modified domes in the second category are near-circular in planform, range from 15 to 30 km, have gently convex upper surfaces which in places have arcuate scarps, and steep flanks with multiple breaks in slope. The third group of modified domes are 15–50 km in diameter, also near-circular in planform often with multiple arcuate scarps, and have flat upper surfaces which have a small depression and pit craters. Modified domes in the fourth category, range from 20 to 50 km in diameter, have elongated or near-circular stellate planforms and extensive upper surfaces, some of which are downsagged. The fifth group of modified domes are near-circular, with diameters ranging between 15 and 60 km with stellate perimeters and have concave inner surfaces.

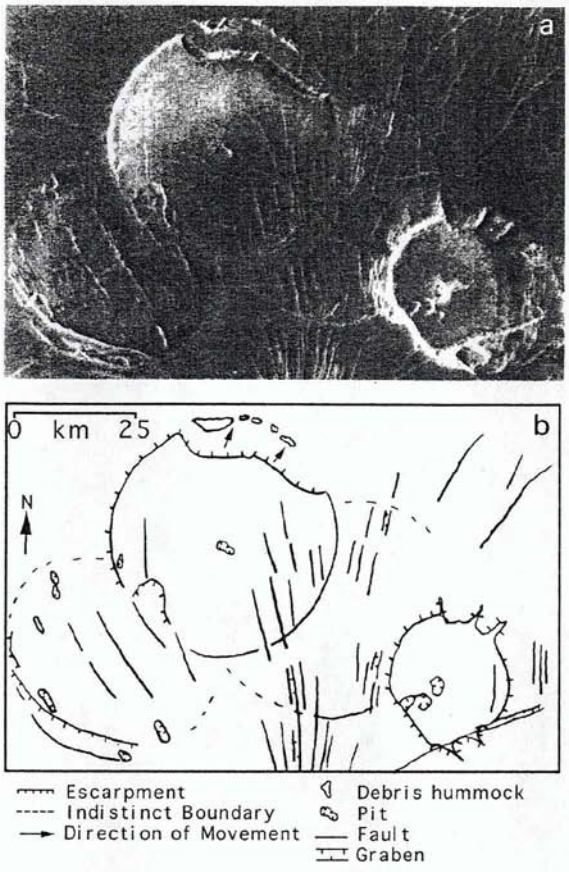

Fig. 2. A range of planimetric forms of modified domes on Venus. Four coalesced domes in Guinevere Planitia (33.6°N, 312°E). The largest dome (MD50 [5]) is 50 km in diameter and has a well defined failure on the northern margin. The smaller dome (MD51 [5]) is 25 km in diameter and has scalloped margins. Radar illumination from the left-side of the image. NASA/JPL Magellan image C1MIDR 30N315.

Volcanic domes are present over most of the planet's surface, >80% of which is made up of volcanic plains. Few domes occur in the highlands or the lowest areas of the plains [5]. Fifty percent of modified domes occur in the volcanic plains and are unassociated with other geological features. A further 31% are associated with coronae [26] and 60% of those are situated in, or on, circumferential fractures bounding such structures. Coronae are postulated to be the surface expressions of mantle upwelling [26]. A total of 17% of domes are associated with large (>100 km in diameter) and intermediate

(20–100 km in diameter) shield volcanoes. Of that total, 47% are situated on the summit region of the volcanoes. A total of 11% of domes are situated in fracture zones. Many of those are heavily modified indicating that the domes were emplaced either prior to the surface fracture formation, or that magma was able to rise to the surface as a result of extensional stresses. Fractures cross-cutting domes indicate that stress continued after emplacement. Tectonic stresses causing dome destruction may also explain why only 3% of the total dome population is associated with tessera, highly deformed upland terrain [19].

5. Comparison of flat-topped seamounts and domes on Venus

Many of the flat-topped seamounts of interest to us on the Hawaiian Ridge, occur west of 163°, for which there is no bathymetry map at present using the GLORIA cruise data. There is bathymetry east of 163°, but it is limited and available only with interpolated 100 m contour spacings making accurate height and slope determinations problematic where the ship did not go right over the summit of a seamount. Therefore, we also compiled data (Fig. 3) of seamounts in the Pacific Ocean in Rano Rahi [27], Gulf of Alaska [32], Emperor [33], Geisha, Michelson and Dutton seamount chains [28]. With the exception of the seamounts in Rano Rahi which tend to be circular or to form volcanic ridges [27], we attempted to obtain information for individual flat-topped stellate seamounts. The diameters of the Hawaiian flat-topped seamounts studied here range from 10 to 60 km which is similar to the range of <5 km to 50 km for seamounts in the other regions we examined. Using the available bathymetric data, typical heights of seamounts studied around

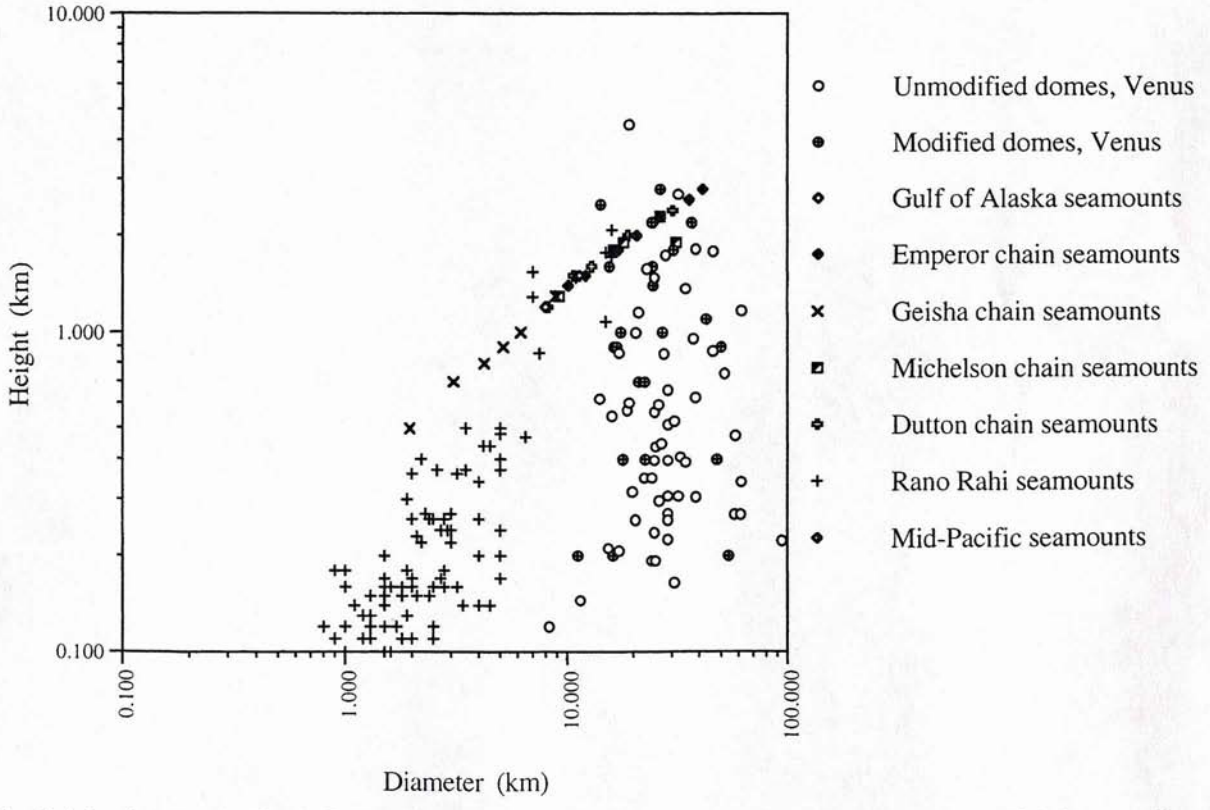

Fig. 3. A log–log plot of edifice height and diameter for a range of seamounts [1,27–31], unmodified and modified domes on Venus [17,8].

the Hawaiian Ridge are ~1000 m (C. Gutmacher, pers. commun.) and slope angles up to the near-horizontal break of slope range between 6° and 30°. Using a height of 1000 m, the volumes of seamounts around the Hawaiian Ridge range from 30 km^3 to 1000 km^3. Seamount volumes in the Rano Rahi Field range from 1–115 km^3 [27], <1–600 km^3 for East Pacific seamounts [29,30], to 10^4–10^5 km^3 for the massive edifices of the Hawaii–Emperor, Dutton, and Michelson chains [33,28]. For point-source volcanism, the volume differences between Rano Rahi seamounts near the southern Eastern Pacific Rise and those in the Hawaii–Emperor chain reflect the higher magma production rates at the Hawaiian hotspot [31]. Volcanoes in the Geisha chain occupy the middle portion of the size spectrum [28].

The average number of radial features per edifice for flat-topped stellate seamounts that have not undergone subaerial erosion is 4 on the Hawaiian Ridge, similar to seamounts in the Emperor, Geisha, Michelson and Dutton seamount chains [31], though Suiko volcano (45°N, 170°E) in the Emperor chain has 10. The average length of radial features around Hawaiian seamounts is <5 km, while in the Geisha chain and Gulf of Alaska seamounts it is 17 km, compared with 64 km for the Michelson chain [31]. The maximum lengths are associated with the largest flat-topped edifices and range from >100 km in the Emperor, Michelson and Dutton chain to <30 km in the Geisha chain (e.g. an extension on Isakou (31°35′N, 151°E) is 16 km long).

Venusian dome diameters measured across the Magellan SAR orbit track range between 10 km and 60 km, the majority being ~20 km. To determine the height of Venusian domes, parallax measurements were made on same-side (Left–Left) and opposite-side (Left–Right) stereo-images using equations from Plaut [34]. Stereo-coverage is limited, and only a few domes have the data coverage necessary for detailed parallax studies. Available compressed-once images (225 m/pixel) were used since global full-resolution (75 m/pixel) data coverage at varying incidence angles does not exist over the domes. The estimated horizontal parallax determination error for the compressed-once data is ±1.5 pixels. Heights of ~900 m and ~1800 m have been determined on two stellate domes. In this study we most frequently calculated the height of a dome based on their observed foreshortening in SAR images and assumed symmetry. This assumption excluded the estimation of the heights of many highly modified domes. However, using this method we determined that height ranges from ~400 m to ~3800 m with a mean height of 1300 m. First-order estimates of volumes of stellate planform domes have been made by assuming a circular planform and truncated conical form. The volumes of Venusian domes range from 10 km^3 to 15,000 km^3 [17,5] which are comparable to those for flat-topped seamounts on the Hawaiian Ridge (30 km^3 to 1000 km^3).

An attempt was also made to estimate the slope of the intact dome margins. On most domes, due to the edifice height and radar viewing geometry, the radar-facing slope is foreshortened, and the backslope is extended. The true width of the dome margin (d_1) was determined using the foreshortened width (d), the height of the dome margin (h) and the radar incidence angle (ϕ):

$$d_1 = d + h/\tan\phi$$

The value of d_1 may then be used to infer a maximum average slope angle for an edifice. We derived a range of slope angles between 20° to 30° on Venus domes. The actual shape (i.e. curvature) of the dome slope remains unknown. The number of radial extensions varies with each modified dome on Venus, but ranges from 2 to 18, with lengths typically <5 km.

6. Interpretation of flat-topped seamount morphologies

From examination of irregular-shaped volcanic ocean islands, it is clear that eruption along radiating volcanic rift zones, pre-existing tectonic structure, caldera collapse, crater and volcano coalescence, slope failure, and erosion are all processes that can modify and control island shapes [35,36]. The range of circular and irregular seamounts around Hawaii indicates that modification of these edifices may also occur by processes similar to those that control ocean islands. Fiske and Jackson [37] recognized that intrusions along rift zones on Hawaii play a significant role in island formation, and sonar images off the coast revealed massive slope failure deposits which

have modified the islands' shape [38]. On Hawaiian volcanoes, there is good seismic and geodetic data that the volcano is not welded to the underlying lithospheric plate, and that intrusive growth is accommodated by spreading along basal decollements [39]. Thrusting over a basal detachment creates a stress state favorable to both slope failures as well as shallow and deep rift zone intrusions [40–43].

Based on work by Fiske and Jackson [37], Vogt and Smoot [31] proposed that seamounts planforms evolve from small and near-circular to larger and stellate due predominantly to the formation of flank rift zones (FRZs). Due to the dependence of rift length on the pressure difference between the base of the magma column below a summit caldera, and hydrostatic pressure at the same level outside the edifice, seamount size is important. Rift development occurs only once a volcano reaches a height of 2 km [44]. Many of the small flat-topped seamounts (1–10 km in diameter) around the Northwest Hawaiian Ridge are only ~1000 m high, yet they have stellate morphologies. Given their small size, it is anticipated that lavas would erupt from a low summit vent rather than along FRZs. While conditions at these seamounts do not favor intrusions, slope failures may be triggered by processes such as overloading of slopes and seismic shaking.

As a seamount builds, increasing load stress occurs both at the summit and at the base [39,40,43]. Seamounts which form on significantly older seafloor, such as those on the Northwest Hawaiian Ridge [1,21], were emplaced onto a layer of sediment and not directly onto the older oceanic crust. During edifice growth, these seamounts can release load stresses by horizontal extension over the layer of sediment on which they are emplaced, which acts as a detachment surface separating the volcanic edifice and the older oceanic crust [39,43]. This favors slope instability as well as the formation and propagation of FRZs, as seen on Hawaii [39,41]. Intrusions into seamounts may trigger slope failures by increasing local pore fluid pressures which act on potential basal failure planes [42,45]. If dike orientations are controlled by the state of stress in the volcano [46], then a large slope failure along a decollement leads to a preferred stress orientation [40] which precludes the formation of symmetric radial dikes. Long linear non-symmetric features, radial to seamounts, and unassociated with mass movement deposits such as occur in the other chains we examined, e.g. the Michelson chain [31], are good evidence for FRZs. However, there is little evidence of such features in the GLORIA images around the Hawaiian Ridge to verify that intrusions have occurred into flat-topped seamounts. This may be due to resolution constraints and masking effects of sedimentation (maximum sonar penetration depth at a 30° grazing angle is 5–30 m [47]).

The GLORIA data show abundant evidence for slope failures around the three categories of seamounts we have examined. Debris aprons around seamounts are characterized by high backscatter acoustic coefficients due to their roughness at the sonar wavelength (Fig. 1). The characteristics of these hummocky aprons are similar to those of aprons off the Hawaiian Islands such as Alika and Nuuanu [38,48]. Several seamounts have large acoustically bright debris aprons containing blocks (>500 m across) that can be traced back to an arcuate backscarps on the flanks of the edifice (Fig. 1). These arcuate backscarps can be seen to form stellate margins on seamounts.

Based on our assessment of flat-topped seamounts on the Hawaiian Ridge and in the Northwest Pacific we propose that the available data support three processes that can form stellate planforms: (1) radial dike intrusions related to flank rift zones; (2) non-radial dike intrusions which cause slope failures; and (3) gravitational slope failures unassociated with intrusions. If stellate margins on small seamounts are the result of intrusions then volcanoes <2 km in height are large enough to initiate FRZs.

7. Interpretation of modified dome morphologies

Head et al. [25] suggested that the stellate planforms of domes on Venus could be the result of radiating dikes, while Bulmer and Guest [8] demonstrated that slope failures can create irregular margins on domes. Based on the observations of the seafloor, we interpret the evidence for dike intrusion in Venus domes. Domes on Venus average <2000 m in height, which on Venus favors the eruption of lavas rather than the formation of a shallow magma chamber and initiation of FRZs, except for

those domes associated with other magmatic centers such as large shield volcanoes [9]. However, stellate domes are abundant throughout the range of elevations and geological settings and their origin needs to be explained. Because of the low erosion rates on Venus and the absence of hydrated, low-permeability sediment layers [49], dome-forming lavas would be emplaced directly onto the volcanic crust resulting in a welded basal boundary condition unlike that which exists for seamounts on the Hawaiian Ridge.

Morphological evidence points to two emplacement scenarios for domes: (1) the circularity of the unmodified domes, coupled with the lack of evidence of break-out flows, suggests emplacement from a central conduit in one continuous event of ductile growth [17,50] where diking would not be favored; and (2) emplacement was either episodic [15], or there were subsequent eruptive events (as indicated by superposed domes). During dome emplacement in either scenario, load stresses would be relieved by horizontal movements until the shear resistance on the margins and base produced horizontal compressive stress in the edifice prohibiting horizontal extension, at which time growth could only continue upwards. Due to the welded boundary conditions on Venus, stress from low lava effusion rates $<10^{-6}$ m^3/s [18], or episodic eruptions could not be accommodated by lateral movement at the dome margins, resulting in brittle deformation or failure within the edifice as well as compression at the base. For those domes associated with mantle upwellings such as coronae [26], localized flexure may occur due to the thinned lithosphere. Evidence in support of this includes circumferential fractures around domes, often inclined steeply towards the dome. Downwarping will cause a change in stress off the periphery of domes from compression to extension in the direction of the downwarping. These zones of extensional stress, if vertical, may favor intrusions, but the SAR data are inconclusive. If the lithosphere at coronae is sufficiently thick to support the weight of a dome then the mantle upwelling [26] may act as an upward load in an equivalent manner to underplating. Such an effect, if present, may support increased load stresses from dome growth, or if regional updoming occurs, cause a reversal of the flexural stress relative to loading from the dome only [49]. As a consequence of regional updoming, extensional stresses

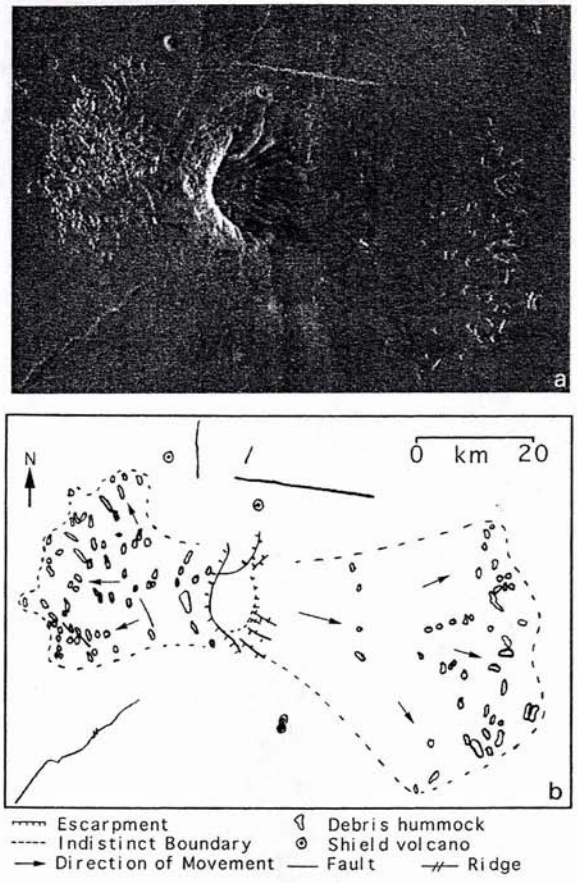

Fig. 4. Two debris aprons associated with a dome (MD33 [5]) in Kawelu Planitia (46°N, 269.5°E) which have characteristic hummocky terrains and lobate planforms [8]. The apron to the east traveled 38 km, is 37 km wide and covers a visible area of 453 km^2. It appears to have been mantled by younger lava flows. The apron to the west, which traveled 26 km, is 25 km wide and covers an area of 515 km^2. Radar illumination from the left-side of the image. NASA/JPL Magellan image C1MIDR 45N265.

will build in the edifice and provide zones of weakness for subsequent intrusions. However, in the case of domes associated with magmatic swells, fractures around many domes which follow the regional extensional stress regime, provide alternative pathways for rising magmas.

Many of the domes appear to have had their circular planforms altered by slope failures (Fig. 4), and radar-bright aprons of materials, rough at the Magellan radar wavelength, occur around the base of the majority of modified domes [5,8]. These aprons contain large blocks (>500 m across) and are similar to

those observed around seamounts and the Hawaiian Islands [38]. The nature of these aprons on Venus, combined with the lack of any evidence that molten lavas were ever exposed during slope failures, indicates that dome failures occurred after they had become solid. There is no evidence in the SAR for more competent rocks being exposed in backscarps, such as would be expected if dikes were involved in the slope failures. If the failures were not triggered by intrusions, then load stresses or seismic shaking may account for them. The integrity of domes may have been compromised by fracturing due to loading stresses or by microcracks and joints formed during cooling. These weaknesses could be exploited by mass rock creep, predisposing the margins to failure. The total effective cohesion or resistance to failure of jointed rock slopes is equal to the combined strength of the blocks and the friction between the joint planes. If stress increases slowly, fracturing occurs progressively, resulting in stress being focused on the remaining intact rock. Once the reduction in strength reaches a point where the average shear resistance is equal to the average shear stress, the slope will fail until it achieves a stable angle. There is clear evidence that slope failures have created irregular margins on domes. For some relict domes all that remains is hummocky terrain.

Based on our observations, the magmatic and tectonic environments in which domes are located do not favor dike intrusions. We propose that the morphologies of domes seen in the SAR data are best explained by emplacement as discrete batches of magma, a mechanism not conducive to intrusions. Due to the welded basal boundary conditions, increased load stress during emplacement can only be accommodated by brittle deformation or failure, processes which weakened the domes. Such weaknesses, along with those from cooling cracks, could be exploited by gravitational creep resulting ultimately in large slope failures. We find that the morphological continuum, from circular to irregular planforms on Venus is best explained by slope failure. There is evidence of older debris aprons occurring near to circular domes which are interpreted to be younger in age than the aprons. We believe that at these sites, the dome from which the debris aprons originated has been eroded and replaced by a subsequent dome-forming episode.

8. Conclusions

Flat-topped seamounts with stellate planforms seen in GLORIA data around the Hawaiian Ridge provide useful analogues to examine the processes that formed modified domes on Venus. We propose that the data for the Hawaiian Ridge and the Northwest Pacific support three processes that can form stellate margins on seamounts:

(1) radial dike intrusion related to flank rift zones;

(2) dike intrusion which cause slope failures;

(3) gravitational slope failure unrelated to intrusions.

The latter processes best explains observations in GLORIA images of small stellate seamounts at the Northwest Hawaiian Ridge. Edifice load stresses can be released by horizontal extension over the sediment layer on which they are emplaced. In the case of Venus, the possibility of intrusions into domes is not favored by the welded basal boundary conditions, plus observations that support dome emplacement as a continuous event of ductile growth. Load stresses could only be relieved by brittle deformation or failure, predisposing the domes to slope failures. Evidence of such slope failures is clearly identifiable in the Magellan SAR data. We conclude that the available data supports modified domes being the product of gravitational slope failures unassociated with intrusions. The existence of extensive debris aprons around volcanoes on the seafloor and domes on Venus indicates that slope failures have a major impact on edifice shape. Slope failures on flat-topped seamounts appear to occur throughout construction and after emplacement has ceased, while on Venus available evidence indicates that slope failures occurred after the domes had solidified. The volumes of debris aprons associated both with seamounts and Venusian domes represent a significant addition to calculations of the total magmas extruded from individual edifices.

Acknowledgements

The authors thank Bruce Campbell, Debbie Smith and Pat McGovern for helpful discussions of this work, and Tracy Gregg, Daniel Scheirer and Nathan Bridges for constructive reviews. Thanks also to

Chris Gutmacher for support and help in using the GLORIA data. *[AC]*

References

[1] R.E. Kayen, M.A. Hampton, J.B. Wilson, D.G. Bishop, Cruise Report: GLORIA Survey of part of the Hawaiian Exclusive Economic Zone, F1-90-HW, U.S. Geol. Surv. Open-File Rep. 90-345 (1990) 53.

[2] S.E.H. Sakimoto, Terrestrial basaltic counterparts for the Venus steep-sided or 'pancake' domes, Lunar Planet. Sci. 25 (1994) 1189–1190.

[3] T. Bridges, Submarine analogs to Venusian pancake domes, Geophys. Res. Lett. 22 (20) (1995) 2781–2784.

[4] D.K. Smith, Comparison of the shapes and sizes of seafloor volcanoes on Earth and 'pancake' domes on Venus, J. Volcanol. Geotherm. Res. 73 (1996) 47–64.

[5] M.H. Bulmer, Small Volcanoes in the Plains of Venus; with Particular Reference to the Evolution of Domes, PhD Thesis, University of London, Senate House, 1994.

[6] J.E. Guest, M.H. Bulmer, J. Aubele, R. Greeley, J.W. Head, G. Michaels, C. Weitz, C. Wiles, Small volcanic edifices and volcanism in the plains of Venus, J. Geophys. Res. 97 (E8) (1992) 15949–15966.

[7] J.B. Wilson, W.R. Normark, Geology of the deep-ocean floor off the Hawaiian Islands from side-scan and swath sonar imaging, 1966–1992, Proc. 5th Int. Congr. History of Oceanography, 1997.

[8] M.H. Bulmer, J.E. Guest, Modified volcanic domes and associated debris aprons on Venus, in: W.J. McGuire, A.P. Jones, J. Neuberg (Eds.), Volcano Instability, Geol. Soc. London, Spec. Publ. 110 (1996) 349–371.

[9] J.W. Head, L. Wilson, Volcanic processes and landforms on Venus: theory, predictions, and observations, J. Geophys. Res. 91 (1986) 9407–9446.

[10] R. Batiza, Seamounts and seamount chains of the eastern Pacific, in: Geology of North America, 5, North East Pacific Ocean Hawaii, Geological Society of America, Boulder, CO, 1989, pp. 289–306.

[11] S.E.H. Sakimoto, M.T. Zuber, The spreading of variable-viscosity axisymmetric radial gravity currents: applications to the emplacement of Venusian 'pancake' domes, J. Fluid Mech. 301 (1995) 65–77.

[12] D. McKenzie, P.G. Ford, F. Liu, G.H. Pettengill, Pancake-like domes on Venus, J. Geophys. Res. 97 (1992) 15967–15976.

[13] N.T. Bridges, J.H. Fink, Aspect ratios of lava domes on the Earth, Moon and Venus, Lunar Planet. Sci. 23 (1992) 159–160.

[14] S.W. Anderson, D.A. Crown, J.P. Plaut, E.R. Stofan, Surface characteristics of steep-sided domes on Venus and terrestrial silicic domes: a comparison, Lunar Planet. Sci. 25 (1994) 33–34.

[15] J.H. Fink, N.T. Bridges, Effects of eruption history and cooling rate on lava dome growth, Bull. Volcanol. 57 (1995) 229–239.

[16] J. Plaut, E.R. Stofan, D.A. Crown, S.W. Anderson, Topographic and surface roughness properties of steep-sided domes on Venus and Earth from radar remote sensing and field measurements, Lunar Planet. Sci. 25 (1994) 1091–1092.

[17] B. Pavri, J.W. Head, K.B. Klose, L. Wilson, Steep sided domes on Venus: characteristics, geological setting, and eruption conditions from Magellan data, J. Geophys. Res. 97 (E8) (1992) 13445–13478.

[18] K.P. Gregg, J.H. Fink, Quantification of extraterrestrial lava flow effusion rates through laboratory simulations, J. Geophys. Res. 101 (1996) 16891–16900.

[19] M.L. Somers, R.M. Carson, J.A. Revie, R.H. Edge, B.J. Barrow, A.G. Andrews, Gloria II — an improved long range sidescan sonar, in: Proc. IEEE/IERE Sub-Conf. Offshore Instrumentation: Oceanology International 78, Technical Session J, London, BPS Publications Ltd., London, 1978, pp. 16–24.

[20] F.F. Sabins, Remote Sensing, Principles and Interpretation, W.H. Freeman, San Francisco, CA, 1978, 426 pp.

[21] B.A. McGregor, E.S. Kappel, J.B. Wilson, J. Campbell, F. Trincardi, R.J. Whittington, W. Mayer, Cruise report, Hawaiian GLORIA leg 7, F10-88-HW, U.S. Geol. Surv. Open-File Rep. 91-333, (1991) 52 pp.

[22] R.S. Saunders, A.J. Spear, P.C. Allin, R.S. Austin, A.L. Berman, R.C. Chandlee, J. Clark, A.V. DeCharon, E.M. De Young, D.G. Griffith, J.M. Gunn, S. Hensley, W.T.K. Johnson, C.E. Kirby, K.S. Leung, G.A. Michaels, J. Miller, R.B. Morris, A.D. Morrison, R.G. Piereson, J.F. Scott, S.J. Shaffer, J.P. Slonski, E.R. Stofan, T.W. Thompson, S.D. Wall, Magellan mission summary, J. Geophys. Res. 97 (1992) 13067–13090.

[23] B.A. Campbell, Use and presentation of Magellan quantitative data in Venus mapping, U.S. Geol. Surv. Open-File Rep. (1995) 95–519.

[24] J.V. Gardner, M.E. Field, H. Lee, B.E. Edwards, D.G. Masson, N. Kenyon, R.B. Kidd, Ground-truthing 6.5-kHz side scan sonagraphs: what are we really imaging?, J. Geophys. Res. 96 (1991) 5955–5974.

[25] J.W. Head, L.S. Crumpler, J.C. Aubele, J.E. Guest, R.S. Saunders, Venus volcanism: classification of volcanic features and structures, associations, and global distribution from Magellan data, J. Geophys. Res. 97 (E8) (1992) 13153–13198.

[26] E.R. Stofan, D.L. Bindschadler, J.W. Head, E.M. Permentier, Corona structures on Venus: models of origin, J. Geophys. Res. 96 (1991) 20933–20946.

[27] D.S. Scheirer, K.C. Macdonald, D.W. Forsyth, Abundant seamounts of the Rano Rahi seamounts field near the southern East Pacific Rise, 15°S to 19°S, Mar. Geophys. Res. 18 (1996) 13–52.

[28] N.C. Smoot, Detailed bathymetry of guyot summits in the north Pacific by multi-beam sonar, Surv. Mapping 43 (1983) 53–60.

[29] D.S. Scheirer, K.C. Macdonald, Near-axis seamounts on the flanks of the East Pacific Rise, 8°N to 17°N, J. Geophys. Res. 100 (1995) 2239–2259.

[30] D.S. Scheirer, K.C. Macdonald, D.W. Forsyth, S.P. Miller, D.J. Wright, M.H. Cormier, C.W. Weiland, A map series of the Southern East Pacific Rise and its flanks, 15°S to 19°S, Mar. Geophys. Res. 18 (1996) 1–12.

[31] P.R. Vogt, N.C. Smoot, The Geisha Guyots: Multibeam bathymetry and morphometric interpretation, J. Geophys. Res. 89 (1984) 11085–11107.

[32] N.C. Smoot, Multi-beam sonar surveys of guyots in the Gulf of Alaska, Mar. Geol. 43 (1981) M87–M94.

[33] N.C. Smoot, Guyots in the mid-Emperor chain mapped with multi-beam sonar, Mar. Geol. 47 (1982) 153–163.

[34] J. Plaut, Stereo Imaging, in: J.P. Ford, J.J. Plaut, C.M. Weitz, T.G. Farr, D.A. Senske, E.R. Stofan, G. Michaels, T.J. Parker (Eds.), Guide to Magellan Image Interpretation, JPL Publ. 93-24, (1993) 33–43.

[35] N.C. Mitchell, Characteristics of irregular coastlines of volcanic ocean islands, Geomorphology 23 (1998) 1–14.

[36] D.J. Fornari, R. Batiza, F. Allan, Irregularly shaped seamounts near the east Pacific rise: Implications for seamount origin and rise axis processes, in: B.H. Keating, P. Fryer, R. Batiza, G.W. Boehlert (Eds.), Seamounts, Islands and Atolls, Am. Geophys. Union Monogr. 43 (1987) 35–48.

[37] R.S. Fiske, E.D. Jackson, Orientation and growth of Hawaiian volcanic rifts: the effects of regional structure and gravitational stresses, Proc. R. Soc., London, Ser. A 329 (1972) 299–326.

[38] J.G. Moore, D.A. Clague, R.T. Holcomb, P.W. Lipman, W.R. Normark, M.E. Torresan, Prodigious submarine landslides on the Hawaiian Ridge, J. Geophys. Res. 94 (1989) 17465–17484.

[39] R.P. Denlinger, P. Okubo, Structure of the mobile south flank of Kilauea, Hawaii, J. Geophys. Res. 100 (1995) 24499–24507.

[40] A. Borgia, J. Burr, L.D. Montero, G.E. Alvarado, Fault propagation folds induced by gravitational failure and slumping of the Central Costa Rica Volcanic Range: implications for large terrestrial and martian volcanic edifices, J. Geophys. Res. 95 (1990) 14357–14382.

[41] B. Van Wyk de Vries, A. Borgia, The role of basement in volcano deformation, in: W.J. McGuire, A.P. Jones, J. Neuberg (Eds.), Volcano Instability, Geol. Soc. London, Spec. Publ. 110 (1996) 95–110.

[42] D. Elsworth, B. Voight, Evaluation of volcano flank instability triggered by dike intrusion, in: W.J. McGuire, A.P. Jones, J. Neuberg (Eds.), Volcano Instability, Geol. Soc. London, Spec. Publ. 110 (1996) 45–53.

[43] P.J. McGovern, S.C. Solomon, State of stress, faulting, and eruption characteristics of large volcanoes on Mars, J. Geophys. Res. 98 (1993) 23533–23579.

[44] H.W. Menard, Geology of the Pacific sea floor, Experimentia 15 (1959) 205–213.

[45] B. Voight, D. Elsworth, Resolution of mechanics problems for prodigious Hawaiian landslides: magmatic intrusions simultaneously increase driving force and reduce driving resistance by fluid pressure enhancement, EOS (1992) 506.

[46] M. Wyss, Hawaiian rifts and recent Icelandic volcanism: expressions of plume generated radial stress fields, J. Geophys. Res. 47 (1980) 19–22.

[47] N.C. Mitchell, A model for attenuation of backscatter due to sediment accumulations and its application to determine sediment thickness with GLORIA sidescan sonar, J. Geophys. Res. 98 (1993) 22477–22493.

[48] W.R. Normark, J.G. Moore, M.E. Torresan, Giant volcano-related landslides and the development of the Hawaiian Islands, in: W.C. Schwab, H.J. Lee, D.C. Twichell (Eds.), Submarine Landslides: Selected studies in the U.S. Exclusive Economic Zone, U.S. Geol. Surv. Bull. 2002 (1993) 184–196.

[49] P.J. McGovern, S.C. Solomon, Filling of flexural moats around large volcanoes on Venus: implications for volcano structure and global magmatic flux, J. Geophys. Res. 102 (1997) 16303–16318.

[50] J.H. Fink, N.T. Bridges, R.E. Grimm, Shapes of Venusian 'pancake' domes imply episodic emplacement and silicic composition, Geophys. Res. Lett. 20 (4) (1993) 261–264.